

## STRENGTH EVALUATION OF ROCKFILL MATERIALS CONSIDERING CONFINING PRESSURE DEPENDENCY

Yoshikazu YAMAGUCHI<sup>1</sup>, Hiroyuki SATOH<sup>2</sup>, Naoyoshi HAYASHI<sup>3</sup>, Hisayuki YOSHINAGA<sup>4</sup>

*1, Dam Structures Research Team(DSRT), Hydraulic Engineering Research Group(HERG),  
Public Works Research Institute(PWRI), 1-6, Minamihara, Tsukuba-shi, Ibaraki-ken, 305-8516, Japan*

*Phone: +81-29-879-6781, Fax: +81-29-879-6737, E-mail: yamaguti@pwri.go.jp*

*2, DSRT, HERG, PWRI, Japan, E-mail: h-sato@pwri.go.jp*

*3, DSRT, HERG, PWRI, Japan, E-mail: nhayashi@pwri.go.jp*

*4, Hydraulic & River Engineering Dept, West Japan Engineering Consultants, Inc.(WEST JEC),*

*1-1-1, Watanabe-dori, Chuo-ku, Fukuoka-shi, Fukuoka-ken, 810-0004, Japan*

*Phone: +81-92-781-1177, Fax: +81-92-781-9599, E-mail: h-yoshinaga@wjec.co.jp*

**Abstract:** It is necessary to evaluate shear strength of rock materials, which are major construction materials for a rockfill dam, considering the confining pressure dependency for the rationalized design and seismic performance evaluation of this dam type. However, the triaxial compression test, which is the most common strength test for rockfill materials, has a problem in test precision under low confining pressure condition.

In this study, we carry out large-scale triaxial compression tests under low confining pressure, large-scale box shear tests, and laboratory surface sliding tests for rock materials. Based on results of these tests, we investigate the evaluation method of the shear strength of rockfill materials under low confining pressure condition. In addition, we make a fundamental study on the setting method of the design strength of rock materials considering the confining pressure dependency.

**Key words:** embankment dam, rockfill materials, design strength, confining pressure dependency

### 1 Introduction

In view of the state of hard condition in the Japanese economy and budget, the cost for dam construction should be reduced based on the results of appropriate research and development. In addition, because there are frequent large earthquakes in Japan, seismic safety evaluation of dams against large earthquake motions is very important. On March 30, 2005, notification regarding the “Draft of Guidelines for Seismic Performance Evaluation of Dams during Large Earthquakes”<sup>[1]</sup> (hereinafter referred to as the “Guidelines”) systematically describing methods of evaluating seismic safety of dams subjected to large-scale earthquakes was given by Ministry of Land, Infrastructure, Transport and Tourism to organizations including all Regional Bureaus. The “Guidelines” specify items regarding basic evaluation methods including earthquake motions used for evaluation and seismic safety to be ensured, as well as methods of seismic safety evaluation by means such as earthquake response analysis.

It is necessary to evaluate shear strength of rock materials, which are major construction materials for a rockfill dam, considering the confining pressure dependency for the rationalized

design and seismic performance evaluation of this type of dam. However, the triaxial compression test, which is the most common strength test for rockfill materials, has a problem in test precision under very low confining pressure condition.

In this study, we carry out large-scale triaxial compression tests under low confining pressure as well as medium and high confining pressures. Besides, we perform large-scale box shear tests, and laboratory surface sliding tests for rockfill materials. Based on the results of these tests, we investigate the evaluation method of the shear strength of rockfill materials under low confining pressure condition. In addition, we discuss the setting method of the design strength of rock materials considering the confining pressure dependency.

## 2 Procedures of laboratory tests

### 2.1 Outline

The first action of this study was to evaluate the compaction properties of the test materials in a laboratory. Following this, large-scale triaxial compression tests and large-scale box shear tests were carried out as laboratory shear strength tests, and then surface sliding tests to evaluate the static angle of repose<sup>[2]</sup>.

### 2.2 Test materials

Two types of test material were used in the laboratory tests: dacite rock materials (hereafter referred to as “Material A”) that is currently used in the construction of a rockfill dam; and an aggregate of crushed stone and crushed sand of sandstone (hereafter referred to as “Material B”). The maximum grain size of both materials was 37.5mm. The grain size distribution curves of each test material is shown in Figure 1. The specific gravity in oven dried condition and water absorption of Material A are 2.391 and 4.66%, theirs of Material B are 2.661 and 0.66%.

### 2.3 Compaction properties of the test materials

Compaction tests were carried out to measure the maximum and minimum densities of the test materials so that the relation between compaction time and relative density could be grasped in each strength test (A full description follows later in the text.). A 37.9kg electric hammer was used for the compaction tool. Each specimen was prepared as follows: the materials were placed in a steel mold, with an inner diameter of 30cm and a height of 60cm up to a thickness of 10cm per layer, vibrated for a given duration each time a new layer was added, and compacted by repeating the procedure up to a depth of six layers.

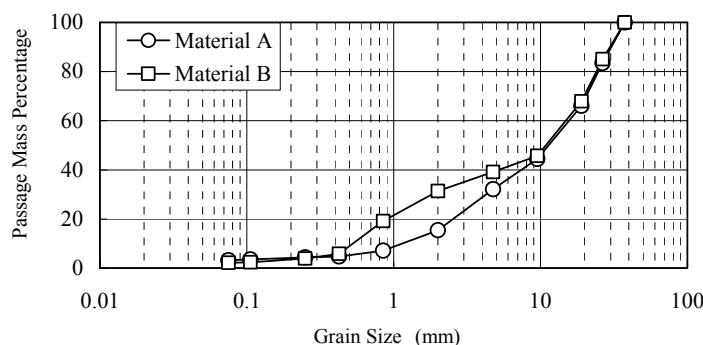


Figure 1 Grain size distribution curves of test materials

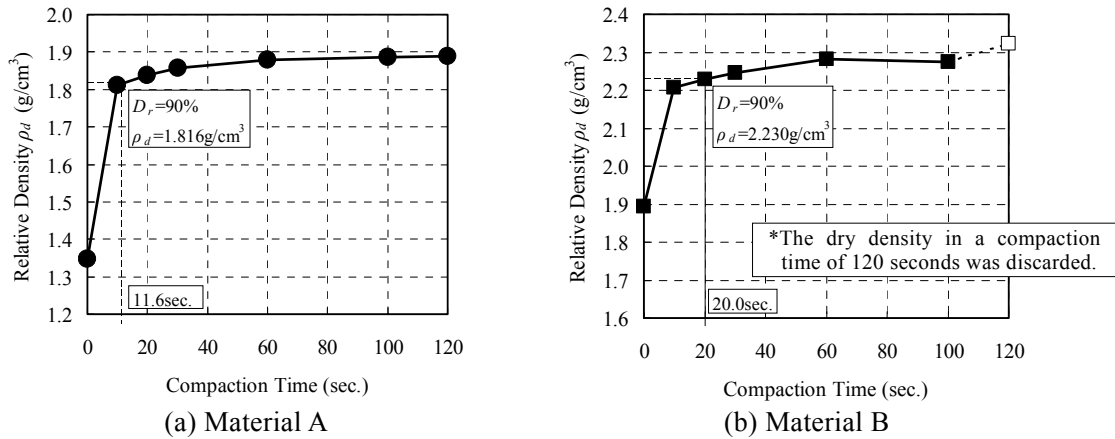


Figure 2 Relation between compaction time and dry density of each test material

Figure 2 shows the compaction test results for each test material. In reference to the relation between compaction time and dry density; in the case of Material A, a minimum dry density,  $\rho_{dmin}=1.348\text{g/cm}^3$ , with a compaction time of zero seconds, and a maximum dry density,  $\rho_{dmax}=1.889\text{g/cm}^3$ , with a compaction time of 120 seconds were adopted. From these test results, a dry density,  $\rho_d=1.816\text{g/cm}^3$ , with a relative density of  $D_r=90\%$  was found to be attainable when the compaction time was 11.6 seconds. As for Material B, a minimum dry density,  $\rho_{dmin}=1.893\text{g/cm}^3$ , with a compaction time of zero seconds and a maximum dry density,  $\rho_{dmax}=2.275\text{g/cm}^3$ , with a compaction time of 100 seconds were adopted. Under these conditions, a dry density,  $\rho_d=2.230\text{g/cm}^3$ , with a relative density of  $D_r=90\%$  was found to be attainable when the compaction time was 20.0 seconds. Thus, for large-scale triaxial compression tests that will be introduced later in the text, the compaction time to satisfy  $D_r=90\%$  was determined as 12 seconds for Material A and 20 seconds for Material B.

## 2.4 Large-scale triaxial compression tests

Large-scale triaxial compression (CD) tests were performed under both saturated and unsaturated conditions under four confining pressures of 49, 98, 196 and 294kPa. In a case of the test under unsaturated condition, air-dried materials were used.

A specimen had a columnar shape with a diameter of 30cm and a height of 60cm. The specimen density was set at  $D_r=90\%$  which was derived from the minimum and maximum densities used in the compaction test. Based on the compaction test results, the compaction time for each layer to satisfy  $D_r=90\%$  was determined as 12 seconds for Material A and 20 seconds for Material B. The material was vibrated for a given duration each time a 10cm-thick layer was added, up to a depth of six layers. The thickness of the membrane was a standard 2mm, which was not calibrated in the evaluation of the test results.

## 2.5 Large-scale box shear tests<sup>[3]</sup>

The large-scale box shear test was also conducted. In terms of the principle of the test method and greater reliability under low confining pressure conditions, this test is less complex than the large-scale triaxial compression test. Figure 3 illustrates the large-scale box shear test equipment used in this study. The principal test requirements are described below.

The tests were performed under both saturated and unsaturated conditions at four normal

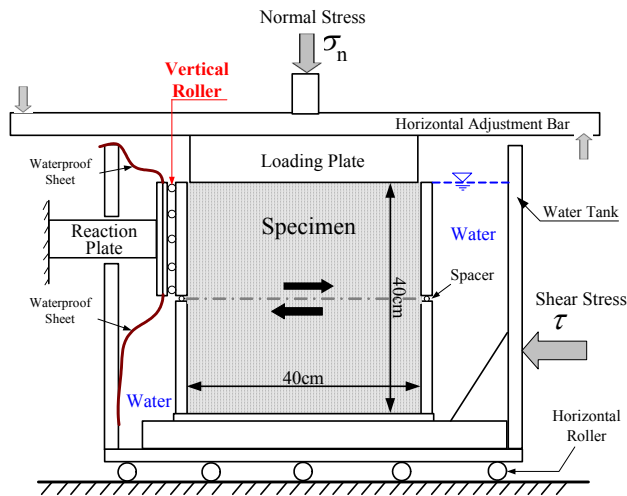


Figure 3 Schematic view of the large-scale box shear test equipment (saturated condition)

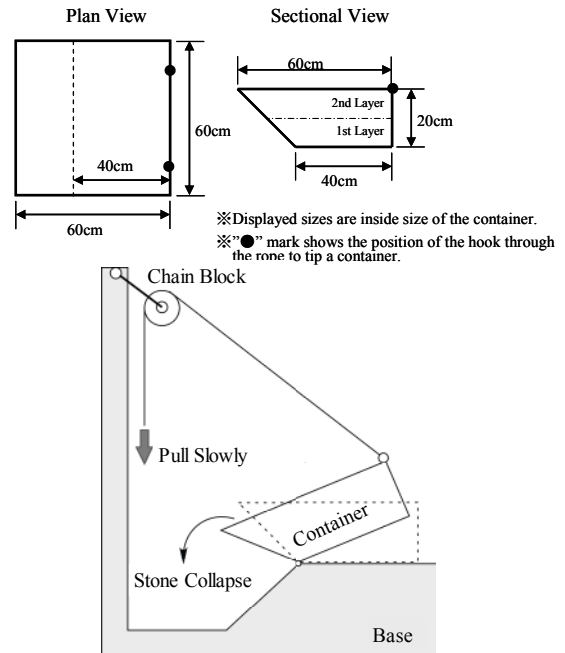


Figure 4 Schematic view of the surface sliding test equipment

stresses of 25, 49, 98 and 196kPa. The normal stress was controlled to remain constant in the shearing process. The specimen was shaped as a 40cm cube. In the test given under saturated conditions, the specimen was placed in a tank, fully immersed in water, as shown in Figure 3.

The materials were vibrated and compacted using the above mentioned electric hammer so that the specimen density of Material A and Material B were  $\rho_d=1.816\text{g/cm}^3$  and  $\rho_d=2.230\text{g/cm}^3$ , respectively, while satisfying  $D_r=90\%$ .

In order to prevent the shear plane of the specimen reaching across its placing joint, the thickness of the first, second and third layers were fixed at 10cm, 20cm and 10cm, respectively. The mass of each individual layer was calculated, based on the volume of each layer and its dry density corresponding to  $D_r=90\%$ , in order to attain the required thickness.

The shear rate was set at 1.3mm/min (approx. 0.3 %/min), which is a strain rate equivalent to the shear rate of 0.2mm/min (approx. 0.3 %/min) in the standard box shear test for a columnar specimen with a diameter of 6cm for sandy soil<sup>[4]</sup>. Regarding the box shear test equipment, there was a concern that the dilatancy of the sheared specimen might cause friction between the shear box and the reaction plate, running the risk of overestimating the shear strength in the calculation<sup>[5]</sup>. In order to reduce friction, vertical rollers were placed between the upper shear box and the reaction plate, as shown in Figure 3. Thus, it should be noted that the box shear test with this test equipment is not a common, but a modified box shear test.

## 2.6 Surface sliding tests

The surface sliding tests were carried out using the equipment shown in Figure 4.

The test materials for the surface sliding tests were prepared by compacting each 10cm-thick layer of two. The materials were compacted evenly over the test container by taking their slope into account. With the aim of assessing changes in the static angle of repose,  $\phi_i$ , with different relative densities, compaction times (0, 5, 10, 20, 30 and 70 seconds) were given to each specimen layer.

This treatment was given to three specimens for each compaction time to obtain an average value. For the calculation of the relative density, the minimum and maximum dry densities obtained in the above compaction tests in **Section 2.3** were employed.

As shown in Figure 4, in the test, the container was gradually tilted by winding up an attached wire on a chain block at a low rate to avoid any impact. The static angle of repose,  $\varphi_i$ , was registered through the observation, as: (i) the angle at which some pieces of material dropped from the specimen; (ii) the angle at which part of the specimen surface started to collapse; (iii) the angle at which the entire surface of the specimen began to collapse, and; (iv) the angle at which the specimen as a whole started to collapse.

### 3 Results of the laboratory tests

#### 3.1 Large-scale triaxial compression tests

The results of the large-scale triaxial compression (CD) tests are shown in Figures 5 and 6. The strength was evaluated in two ways: the common method based on the Mohr-Coulomb's failure criterion; and the  $\varphi_0$  method by obtaining a straight line passing through the origin of the coordinate axes and tangent to Mohr's circle under each confining pressure. The following are their relational expressions.

$$\text{Mohr-Coulomb's failure criterion: } \tau_f = c + \sigma_n \tan \varphi \quad (1)$$

$$\varphi_0 \text{ method: } \tau_f = \sigma_n \tan \varphi_0 \quad (2)$$

where,  $\tau_f$ : shear strength,  $c$ : cohesion,  $\sigma_n$ : normal stress on shear plane,  $\varphi$ : internal friction angle, and  $\varphi_0$ : internal friction angle under each confining pressure with the cohesion of  $c=0$ .

According to the test results, the strength of both Material A and Material B was slightly greater in an unsaturated condition than in a saturated condition. The internal friction angle of the material

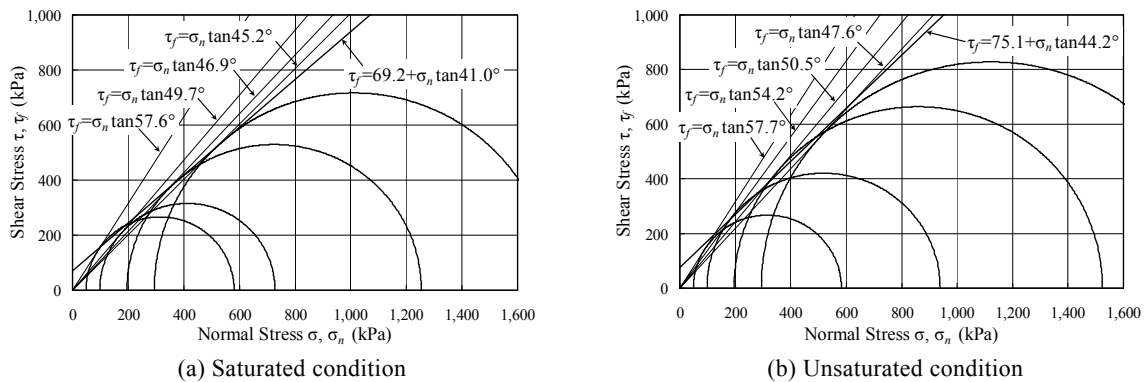


Figure 5 Results of the large-scale triaxial compression (CD) test for Material A

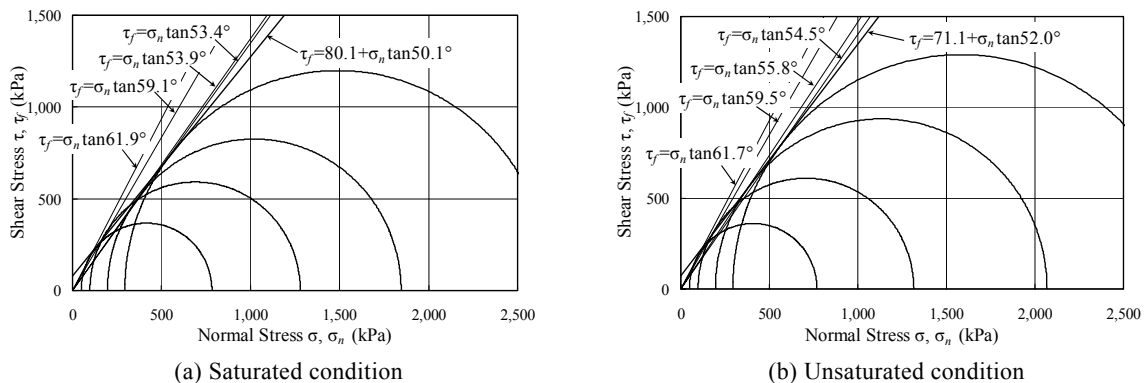


Figure 6 Results of the large-scale triaxial compression (CD) tests for Material B

obtained from a strength line on the basis of the Mohr-Coulomb failure criterion is greater in an unsaturated condition than in a saturated condition by as much as 2° to 3°, where the difference in cohesion is negligible. In comparison with the  $\varphi_0$  method, a similar degree of strength was observed at the lowest confining pressure of 49kPa. But, as the confining pressure increases, the value in the saturated condition reduces by as much as 3° to 5° for Material A and 1° to 2° for Material B.

Material B is 4° to 9° greater in  $\varphi_0$  and 8° to 9° greater in  $\varphi_d$  than Material A. This may be because Material B is assumed to contain very sound and solid crushed stone and sand.

### 3.2 Large-scale box shear tests

The results of the large-scale box shear tests are shown in Figure 7. The strength constants,  $c$  and  $\varphi$ , derived from the approximate line in accordance with the Mohr-Coulomb failure criterion are indicated. In Figure 7, the internal friction angle for both Materials A and B is greater in the unsaturated condition than in the saturated condition by nearly 3°.

Because rollers were installed to reduce the friction between the reaction plate and the shear box, it was assumed that dilatancy in the shearing process might induce the upheaving of the specimen and the shear box together and that the shear plane might actually withstand not only normal stress but also the weight of the upper shear box. Thus, in obtaining the shear strength constants of  $\varphi_0$ ,  $c$  and  $\varphi$ , the calculation of normal stress was modified by adding the stress of the shear box weight to the normal stress loaded as test equipment. For the test in the saturated condition, the weight equivalent to the buoyancy of the upper shear box was deducted.

In order to confirm the consistency of box shear test results and triaxial compression test results, a comparison is made in Figure 8, through the curvature failure criterion (hereafter referred to as the “ $Ab$  method”) that takes the confining pressure dependency of the shear strength of rock materials into account. The  $Ab$  method can be expressed with Equation (3)

$$\tau_f = A(\sigma_n)^b \quad (3)$$

where,  $\tau_f$  : shear strength,  $\sigma_n$ : normal stress on a sliding surface (effective stress),  $A$  and  $b$ : coefficients obtained from the test results.

From Figure 8, the results of the box shear tests for both Materials A and B under saturated and unsaturated conditions were found to have a significantly high correlation with the results of the triaxial compression tests in this study, for which it is almost possible to draw a single curve of shear strength. It was proved that the measure of eliminating friction around the shear box of the

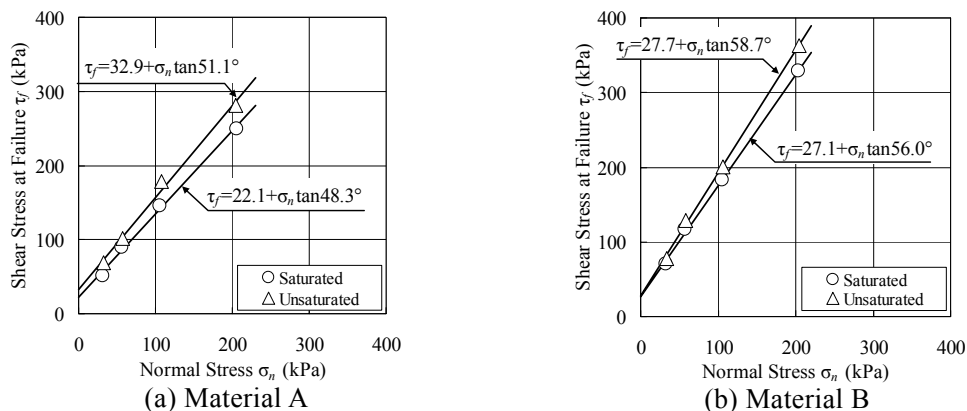


Figure 7 Relation between normal stress and shear stress at fracture based on the results of the large-scale box shear tests

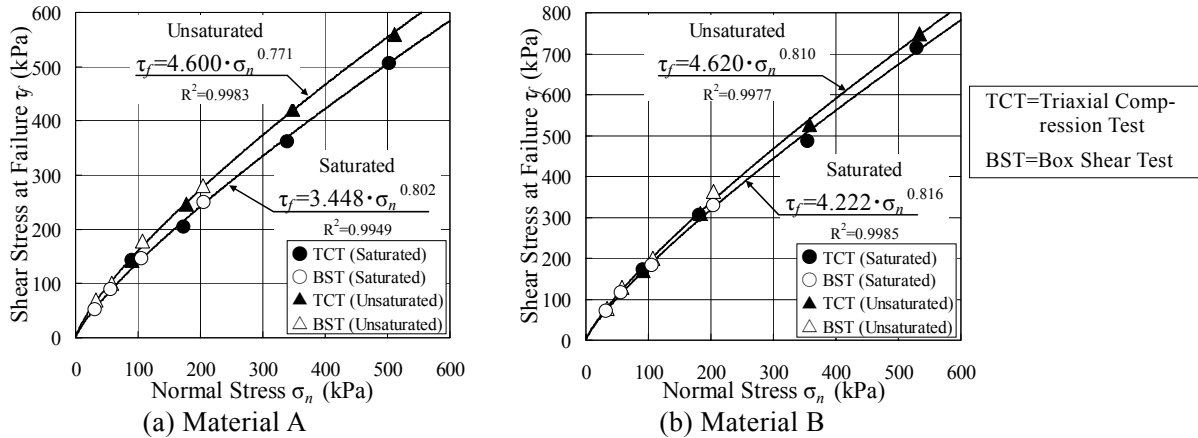


Figure 8 Comparison of the shear strength between box shear tests and triaxial compression test equipment was effective, making it possible to attain results similar to those in the triaxial compression test. Furthermore, this modified box shear test enables an evaluation of shear strength under a confining pressure below 50kPa, a result unattainable with the triaxial compression test.

### 3.3 Surface sliding tests

The results of the surface sliding tests are summarized in Table 1. From these results, the compaction time appropriate for this test equipment was established at approximately five seconds for Material A and ten seconds for Material B when the condition of  $D_r=90\%$  or over was satisfied, and the test results were comparable to the triaxial compression test and the box shear test. Then,  $\phi_0$  obtained from the results of both the triaxial compression test and box shear test, together with the static angle of repose,  $\phi_i$ , that was obtained from the surface sliding test in the above mentioned compaction time and equivalent to the internal friction angle, were plotted on the same graph as can be seen in Figure 9. The numbers (i) through (iv) on the right shoulder of the surface sliding test results correspond with the static angles of repose in the situations (i) through (iv) listed in Table 1. This diagram reveals that the static angle of repose for both materials in situation (ii) is equal to the internal friction angle,  $\phi_0$ , under the confining pressure of 49kPa (about 90kPa if converted into normal stress) in the triaxial compression test and under normal stress between 50 and 98kPa (between 58 and 107kPa after conversion) in the box shear test, and that the value of  $\phi_0$  under the normal stress of 25kPa (about 33kPa after conversion) in the box shear test remains between the situations (ii) and (iii). If a logarithmic curve, which is drawn to link the triaxial compression test results with the box shear test results, is extended toward the lower confining pressure side, the

Table 1 Results of surface sliding tests

Compaction Time (sec.)	Material A					Material B				
	Relative Density $D_r$ (%)	Static Angle of Repose $\phi_i$ (°)				Relative Density $D_r$ (%)	Static Angle of Repose $\phi_i$ (°)			
		Situation(i)	Situation(ii)	Situation(iii)	Situation(iv)		Situation(i)	Situation(ii)	Situation(iii)	Situation(iv)
0	25.2	31.8	41.1	45.1	54.6	21.8	35.9	43.7	47.6	52.8
5	93.3	48.8	61.3	68.5	72.1	84.0	47.3	unidentified	62.2	73.9
10	98.0	54.3	63.5	68.4	70.3	91.9	51.9	61.5	71.5	not collapse
20	103.3	57.5	67.7	70.8	74.9	96.3	49.2	64.7	70.7	not collapse
30	102.8	54.7	65.2	70.6	73.4	95.4	45.3	62.5	66.4	74.4
70	109.3	56.1	65.1	71.1	not collapse	88.4	49.0	57.3	65.1	65.9

Situation (i): the angle at which some pieces of material drop from the specimen  
 Situation (ii): the angle at which part of the surface of the specimen starts to collapse  
 Situation (iii): the angle at which the entire surface of the specimen starts to collapse  
 Situation (iv): the angle at which the specimen as a whole starts to collapse

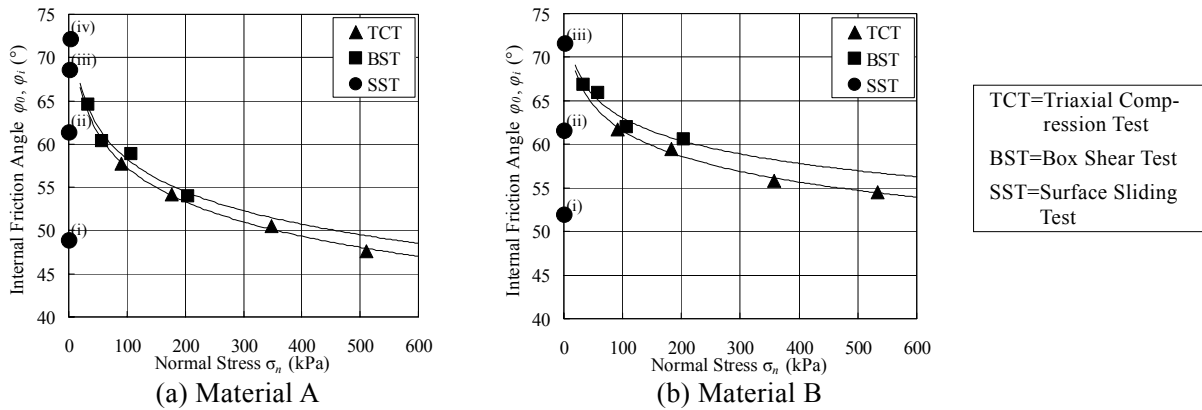


Figure 9 Comparison of results between triaxial compression tests, box shear tests and surface sliding tests

values for both Materials A and B approximate the static angle of repose in the situation (iii) of the surface sliding test. The situation (iii) where the entire specimen surface collapses is considered to be the most appropriate state in evaluating the strength at fracture. Based on these results, in order to evaluate the shear strength of any rock material under a low confining pressure where the normal stress is significantly low, it is suggested that the static angle of repose in the situation (iii) of the surface sliding test introduced in this study be assessed.

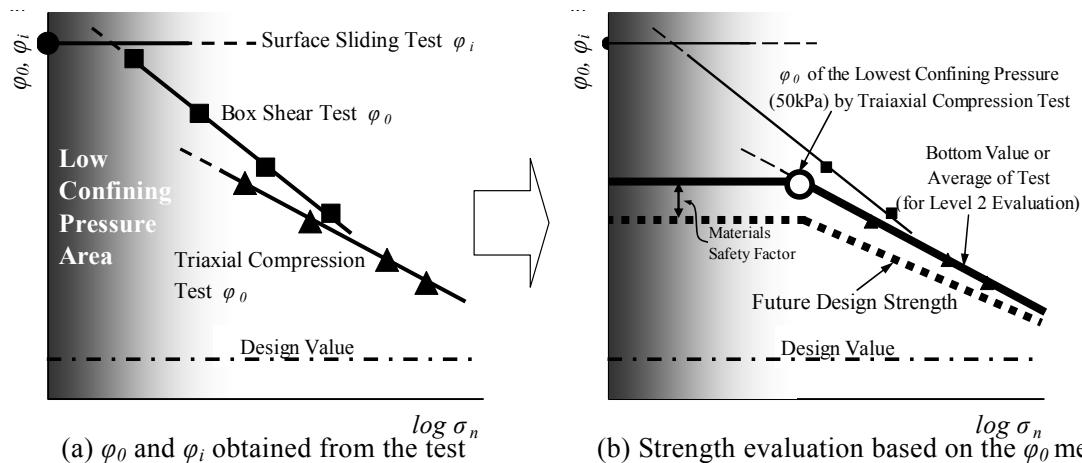
#### 4 Strength evaluation of rock materials under low confining pressure and establishment of practical design strength

Based on the findings of this study, the evaluation of the internal friction angle of rock materials with the consideration of confining pressure dependency and low confining pressure range, as well as the practical formulation of the design strength are explained in Figure 10. The internal friction angle,  $\varphi$ , in the figure was derived from the triaxial compression test results and the box shear test results using the  $\varphi_0$  method. The factor of  $\varphi_i$  in the surface sliding test is equivalent to  $\varphi_0$  under considerably low confining pressure.

First, using the triaxial compression test, which is the most common strength test for rock materials,  $\varphi_0$  of rock materials under each confining pressure condition is found. However, because performing the triaxial compression test under a confining pressure below 50kPa carries it with certain difficulties, the box shear test and the surface sliding test are conducted to obtain the internal friction angles,  $\varphi_0$  and  $\varphi_i$ , in a low confining pressure range. If the resultant  $\varphi_0$  and  $\varphi_i$  are confirmed to be equivalent to or greater than the  $\varphi_0$  derived from the triaxial compression test under the lowest confining pressure of 50kPa, it may be possible to adopt the strength setting method by  $\varphi_0$  as the strength in a confining pressure range below 50kPa.

In this manner, by finding the internal friction angle through the  $\varphi_0$  method, the strength setting method can apply the lower limit or the average of several test values to the seismic performance evaluation for rockfill dams against Level 2 earthquake motions. Furthermore, its method can integrate the lower limit of test values into the future practical design as the design strength allowing for material anomalies and material safety factor based on test accuracy. The validity and exact values of material safety factors, however, need to be closely examined together with the stability analysis.

Based on the above findings, the shear strength obtained from the laboratory tests and field tests



(a)  $\phi_0$  and  $\phi_i$  obtained from the test (b) Strength evaluation based on the  $\phi_0$  method  
 Figure 10 Evaluation of the internal friction angle of rock materials with the consideration of confining pressure dependency and low confining pressure range, as well as the concept of establishing the design strength

on Materials A and B will be evaluated, and the strength evaluation method will be examined.

Among all the tests given to Materials A and B, for those compacted specimens under the unsaturated condition, the relation between the normal stress on shear plane,  $\sigma_n$ , and the internal friction angle ( $\phi_0$  or  $\phi_i$ ) is shown in Figure 11. According to the diagram, the box shear test is able to yield results under low confining pressure that the triaxial compression test is not applicable, and such results can be considered to remain on extension of the  $\phi_0$  result obtained from the triaxial compression test. Thus, it may become possible to increase the strength of the rock materials down to a range of considerably low confining pressure, as long as the box shear test is carried out under a low confining pressure in tandem with the triaxial compression test. Furthermore, with the additional surface sliding test results, the angle of repose can be plotted on an extension of the shear test result in a low confining pressure range which the laboratory shear test cannot achieve, suggesting considerable high shear strength around the surface of rock materials for rockfill dams.

In Figure 11, if we see  $\phi_0$ , which was obtained from the triaxial compression test and dependent on confining pressure, as a base value, we recognize that box shear test results and surface sliding test results are equivalent to or greater than  $\phi_0$  that was derived from the triaxial compression test under the lowest confining pressure. Thus, from the design safety standpoint, it may be possible for us to apply  $\phi_0$ , which has been yielded under the lowest confining pressure in the triaxial compression test, to the strength setting in a low confining pressure range.

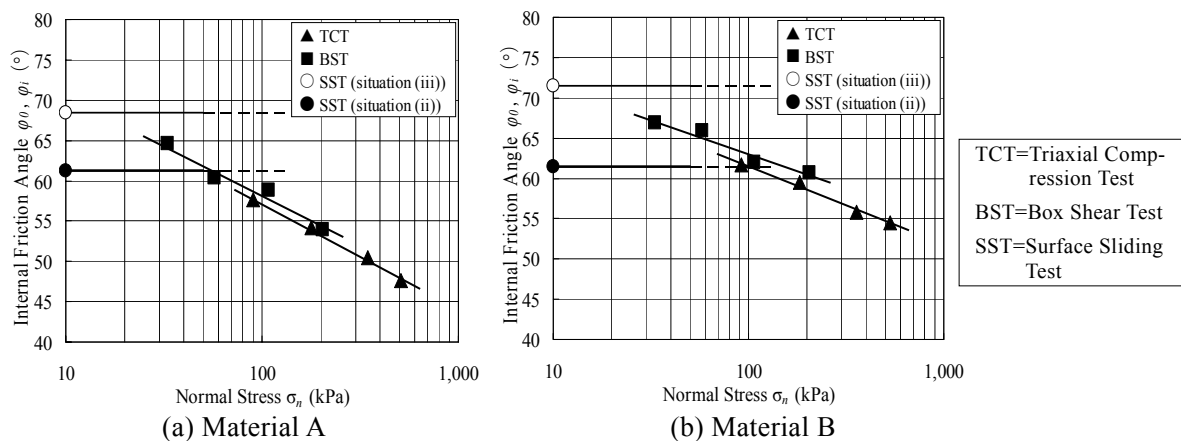


Figure 11  $\sigma_n$ - $\phi$  relationship

## 5 Conclusions

In this study, for the purpose of examining the strength evaluation for rock materials under low confining pressures, laboratory tests such as the large-scale triaxial compression test, the large-scale box shear test and the surface sliding test were carried out. As a result, the following findings were obtained.

- (1) The internal friction angle,  $\varphi_0$ , calculated in the  $\varphi_0$  method by using a large-scale triaxial compression (CD) test result, was confirmed to have a property of confining pressure dependency where the angle decreases as the confining pressure increases, regardless of material types and whether the specimen is saturated or unsaturated.
- (2) Regardless of material types and whether the specimen is saturated or unsaturated,  $\varphi_0$  was confirmed to be far greater than the internal friction angle,  $\varphi_d$ , which is calculated in the Mohr-Coulomb's failure criterion.
- (3) As a measure to mitigate ambient friction, a modified large-scale box share test equipment was constructed by installing rollers between the upper shear box and the reaction plate. As a result, it was clarified that the large-scale box shear test can produce shear strength at a level similar to that of the large-scale triaxial compression test under the same normal stress (confining pressure), regardless of material type and whether the specimen is saturated or unsaturated, and can evaluate shear strength under a confining pressure lower than 49kPa, which is considered to be the verification limit of the large-scale compaction test.
- (4) Notwithstanding the lower test accuracy in comparison with the large-scale triaxial compression test and the large-scale box shear test, the surface sliding test makes it possible to calculate the angle of repose corresponding to the internal friction angle under considerably low confining pressures.

Based on the above test results, some propositions are given in **Chapter 4** for practical methods of establishing design strength of rock materials that could see employment in the rational design of rockfill dams in the future and for reference strength that could be used in the seismic performance evaluation.

## References

- [1] River Bureau, Ministry of Land, Infrastructure, Transport and Tourism, Guidelines for Seismic Performance Evaluation of Dams during Large Earthquakes (draft), Mar. 2005. (in Japanese)
- [2] Yamaguchi, Y., Hayashi, N. and Yoshinaga, H. Fundamental Study on Design Strength of Rockfill Materials Considering Dependence of Confining Pressure, Engineering for Dams, No.261, June 2008. (in Japanese)
- [3] Yamaguchi, Y., Satoh H., Hayashi, N., Yoshinaga, H., Sreng, S. and Shimomura, S. Development of Large-scale Box Shear Apparatus for Coarse-grained Materials of Rockfill Dams, The 43<sup>rd</sup> Japan National Conference on Geotechnical Engineering, July 2008. (in Japanese)
- [4] Japanese Geotechnical Society, Method and Instruction of Soil Tests, Mar. 2000. (in Japanese)
- [5] Society of Soil Mechanics, Deformation and Strength of Coarse Grained Materials, May 1986. (in Japanese)